

# EXPERIMENTAL STUDY OF STATISTICS OF RANDOM WAVES PROPAGATING OVER A BAR

Yuxiang Ma<sup>1</sup>, Guohai Dong<sup>2</sup> and Xiaozhou Ma<sup>3</sup>

A series of physical experiments on the variations of statistics of random waves propagating over a submerged bar were conducted. Random waves were generated by JONWSAP spectra, varying initial spectral width but fixing the wave height and peak frequency. It is found that some freak waves can be formed in the shoaling region close to the top of the bar. And the appearance of these freak waves are mainly caused by the local triad wave-wave interactions. In addition, the probability occurrence of the freak waves has negligible relation with the spectral width. Additionally, the appearance of freak waves is relating to the increasing of wave groupiness in the shoaling region. Furthermore, the relationship between the skewness and kurtosis in the shoaling region can be predicted well with the formula by Mori and Kobayashi (1998).

*Keywords: random waves, wave statistics, freak waves, wavelet transform*

## Introduction

Wave behaviors play a critical role in determining the design of coastal structures and for description of many coastal processes (Goda, 2010). Hence, a clear understand of wave characteristics, in particular the probability of occurrence for huge waves, is urgent in the nearshore zone. Sudden appearance of extreme large waves can cause severe damage of structures and human casualties (Dysthe et al., 2008). In deep water, the occurrence of freak waves is closely related to wave statistics, such as kurtosis and skewness, such as kurtosis and skewness (Mori and Janssen, 2006). However, recent studies (Zeng and Trulsen, 2012; Trulsen et al., 2012; Sergeeva et al., 2011) found that, when waves propagate over a slope bottom, the skewness and kurtosis can reach to a maximum value near the shallower side of a slope and extreme waves can be formed. Kashima et al. (2013) also pointed out freak waves can be generated by the shoaling effect. Katsardi et al. (2013) experimentally found out that in shallow water large waves, which cannot be described by any existing wave height distributions, can be formed. In the field observations (Chien et al., 2002; Nikolkina and Didenkulova, 2011; Wang et al., 2013), freak waves are also identified in coastal region. Hence, research on the predication of the appearance of these extreme waves and the behind mechanics is crucial in coastal engineering.

Investigation of waves propagating over a submerged bar is a good way to assess the wave behaviors in coastal region (Beji and Battjes, 1993). The purpose of this study is to study the statistics (variation, groupiness, kurtosis and skewness) changes of random waves over a submerged bar. Particularly, the relation between the statistics and the occurrence of extreme waves is the primary target.

## Experimental setup

The experiment was conducted in a wave flume located in the state key laboratory of coastal and offshore engineering, Dalian University of Technology. This wave flume is 50.0 m long, 3.0 m wide and 1.0 m depth. In the present study, the water depth is  $h = 0.45$  m. A submerged isosceles trapezoidal bar with slopes of 1:20 and a 3m horizontal crest was constructed. The detail experimental setup is shown in Figure 1.

Random wave simulations based on JONSWAP spectra with constant significant wave height  $H_s$  and constant peak frequency  $f_p$ , but different peak enhancement factor  $\gamma$ . The detailed wave parameters are shown in Table 1. As the width of the flume is 3.0 m, which was longer than the primary wave length used in this study, the cross-tank modulation may be occurred. Hence, to ensure two-dimensionality of the wave field, a surface-ground steel wall was installed to separate the flume longitudinally into two sections with widths of 0.8 m and 2.2 m. The narrower 0.8-m-wide section was chosen as the working section (Figure 2).

The water surface elevations were recorded by means of capacitance-type wave gauges at 17 different locations along the flume. To obtain enough samples for a statistics analysis, 20 realizations of the random waves with the same imposed spectrum were generated with different sets of random phases. For each experimental cases, 200s time series were collected, hence, about 4200 individual waves were measured at each location.

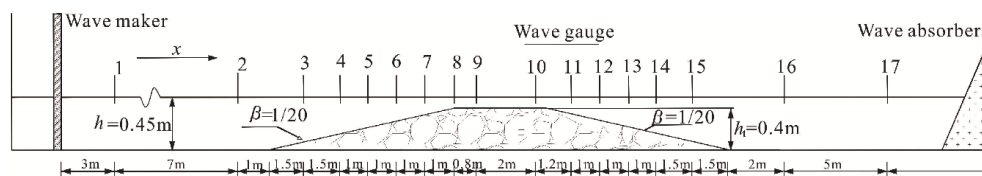


Figure 1. Schematic drawing of the experimental set

1 State key laboratory of coastal and offshore engineering, Dalian University of Technology, Dalian, 116023, China  
2. State key laboratory of coastal and offshore engineering, Dalian University of Technology, Dalian, 116023, China  
3. State key laboratory of coastal and offshore engineering, Dalian University of Technology, Dalian, 116023, China



Figure 2. Photo of the experimental setup

Case	$f_p$ (Hz)	$H_s$ (m)	$\gamma$
1	1.0Hz	0.049	1.5
2			3.3
3			5
4			7

### Wavelet Analysis

The continuous wavelet transform  $WT(a, \tau)$  of a time series  $\eta(t)$  is defined as (Torrence and Compo, 1998):

$$WT(a, \tau) = \int_{-\infty}^{\infty} \eta(t) \psi_{a,\tau}^*(t) dt, \quad (1)$$

where the asterisk denotes the complex conjugate, and  $\psi_{a,\tau}(t)$  represents a family of functions called wavelets that are constructed by translating in time,  $\tau$  and dilation with scale,  $a$ , a mother wavelet function  $\psi(t)$ . The scale  $a$  can be interpreted as the reciprocal of frequency,  $f = 1/a$ . The  $\psi_{a,\tau}(t)$  expression is defined as:

$$\psi_{a,\tau}(t) = |a|^{-0.5} \psi\left(\frac{t-\tau}{a}\right). \quad (2)$$

One of the most extensively used mother wavelets in ocean engineering is the Morlet wavelet; it is a plane wave modulated by a Gaussian envelope and is defined as:

$$\psi(t) = \pi^{-1/4} \exp\left(-\frac{t^2}{2}\right) \exp(i\omega_0 t), \quad (3)$$

where  $\omega_0$  is the peak frequency of the wavelet, usually chosen to be 6.0 (Farge, 1992).

Through the wavelet coefficients,  $WT(a, \tau)$ , one can defined the local wavelet energy density or scale-averaged wavelet power,  $W(\tau)$ :

$$W(\tau) = \int_0^{\infty} \frac{|WT(a, \tau)|^2}{a} da, \quad (4)$$

Dong et al. (2008) proposed a groupiness factor ( $GF$ ) by  $W(\tau)$  to quantify the groupiness of wave trains:

$$GF = \sqrt{\frac{1}{T} \int_0^T [W(t) - \overline{W(t)}]^2 dt / \overline{W(t)}}, \quad (5)$$

where  $\overline{W(t)}$  is the mean of  $W(t)$  over time,  $T$  is time length of the series.

The wavelet based bispectrum is defined as:

$$B(f_1, f_2) = \int_{\tau} \{WT(f_1, \tau) WT(f_2, \tau) WT^*(f, \tau)\} d\tau, \quad (6)$$

where  $x(t)$  and  $y(t)$  are the time series embedded in the respective  $WT_s$ , and  $f_1, f_2$  and  $f$  must satisfy the frequency sum rule:

$$f = f_1 + f_2. \quad (7)$$

The bispectrum measures the amount of phase coupling in the interval  $T$  that occurs between wavelet components of scale lengths  $a_1$  and  $a_2$  of  $x(t)$  and wavelet component  $a$  of  $y(t)$  in a manner such that the sum rule is satisfied. The real part of  $B$  relates to wave skewness ( $S$ ) and the imaginary part of  $B$  contributes to wave asymmetry ( $A$ ):

$$S = \frac{\sum \sum \text{Re}\{B(f_1, f_2)\}}{E(\eta(t)^2)^{3/2}}, \quad (8)$$

$$A = \frac{\sum \sum \text{Im}\{B(f_1, f_2)\}}{E(\eta(t)^2)^{3/2}}, \quad (9)$$

where  $E$  denotes the expected value.

If the imaginary part of  $B$  is positive, then energy is transferred from the  $a_1$  and  $a_2$  components to a component. For negative imaginary part of  $B$ , the energy transfer reverses and the  $a_1$  and  $a_2$  components grow at the expense of a component (Herbers et al., 2000).

To directly measure the degree of nonlinear phase coupling, the normalized wavelet bispectrum or called the wavelet bicoherence is usually used (Dong et al., 2008; Ma et al., 2010):

$$b = \frac{B(f_1, f_2)}{\left[ \int_T |WT(f_1, t) WT(f_2, t)| dt \right] \int_T |WT(f, t)| dt}, \quad (10)$$

The value of bicoherence is between -1 and 1, and represents the relative degree of phase coupling between triads of waves. For example, with  $b = 1$  for a maximum amount of coupling and  $b = 0$  for random phase relationships.

### Results and Discussion

Segments of the measured surfaces elevations of Case 1 at six different locations along the flume are shown in Figure 3. The wave profiles are asymmetric about mean water with their crests sharper than their troughs as expected on the upslope side due to the shoaling and the nonlinear wave-wave interactions effects. Some large waves are formed during this process. For example, the wave surface elevations measured at  $x = 15\text{m}$  (as shown in Figure 3), the maximum crest around  $t = 163\text{s}$  reach to 6.4cm, which is larger than the 1.25 times of the background significant wave height, satisfying the definition of freak waves (Dysthe et al., 2008). Over the crest of the bar, the wave profiles become symmetrical with respect to both the horizontal and the vertical axis owing to the release of some bound higher harmonics and the deshoaling effect.

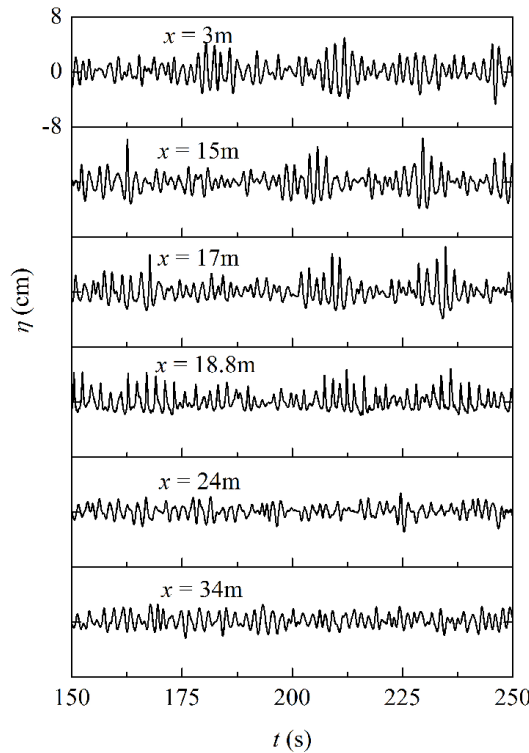


Figure 3. Segments of the surface elevations for Case 1 measured at different location.

The probability occurrence of freak waves for each experimental case is shown in Table 2. It is found that maximum probability of occurrence of freak waves occurred at the region close to the top of the bar (No. 7 probes location). After wave breaking, the number of freak waves reduces dramatically. The results shown in Table 2 also indicate that wave trains with the averaged  $\gamma$  ( $\gamma = 3.3$ ) are most likely to induce freak waves. Wave trains with the smaller  $\gamma$  (Case 1,  $\gamma = 1.5$ ) have the least possible to generate freak waves. It is interesting to note that the probability occurrence of freak for wave trains with narrower bandwidth (i.e. larger  $\gamma$ ) is smaller than the wave trains with  $\gamma = 3.3$ , indicating that the formation mechanism of freak waves in shallow water is quietly different from that in deep water. In deep-water condition, wave trains with narrower bandwidth have the largest probability occurrence of freak waves (Mori and Janssen, 2006).

**Table 2. Probability of occurrence of freak waves**

Note:  $N_T$  is the measured total wave number,  $N_F$  is the identified freak wave number and  $P_F$  is the probability of occurrence of freak waves ( $\eta_c > 1.25H_s$ ).

Case	$N_T$	$N_F(7\#)$	$P_F(7\#)$	$N_F(8\#)$	$P_F(8\#)$
1	4514	5	0.11%	2	0.044%
2	4345	21	0.48%	4	0.092%
3	4230	9	0.21%	2	0.047%
4	4177	10	0.24%	2	0.048%

Figure 4 gives an illustration of the occurrence of a freak wave in a wave train measured at the upslope side near the crest of the bar. Meanwhile, the corresponding wavelet spectrum is also presented. It is shown that, at the time of freak wave occurrence, the higher harmonics are very dense. The higher harmonics are almost in-phase with the local primary waves, suggesting that the higher harmonics are locked by the primary waves. The wavelet spectrum reveals that the formation of freak waves on the upslope is mainly caused by superimposing the primary waves and the corresponding higher harmonics. After wave breaking, the locked higher harmonics are released and are de-phasing with the primary wave. Combined with the dissipation effect, the number of freak waves decreased.

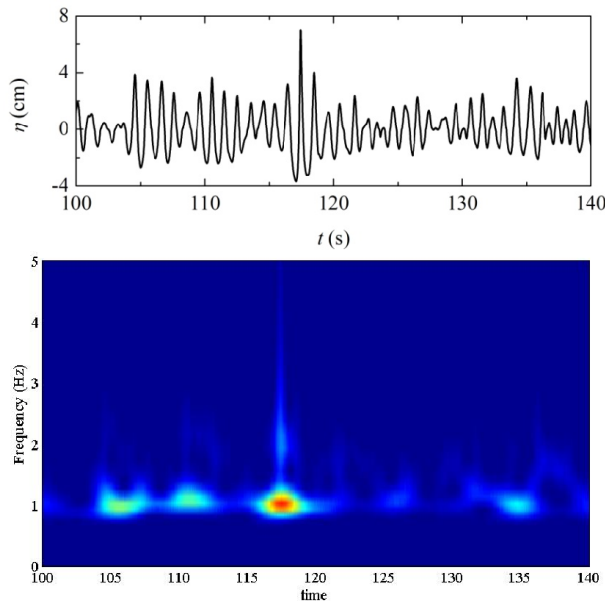


**Figure 4. A demonstration of a freak wave in wave series (the upper panel) and the corresponding wavelet spectrum (the lower panel).**

To expose the behind mechanism, the wavelet-based bicoherence (Dong et al., 2008) is adopted to investigate the nonlinear phase coupling occurring in the wave series. The bicoherence spectra for all the surface elevations (20 realization) measured at the No. 7 location for the experimental case 2 is shown in Figure 5. Meanwhile, the bicoherence for one realization also illustrated. It is found that the values of the imaginary part of the bicoherence of the primary and higher harmonics are positive but small, indicating that the local energy transfer to the higher harmonics is limited for the whole series. The values of bicoherence of the realization with the maximum number of freaks waves are larger than the whole series for both the real and imaginary parts, suggesting the higher harmonics mainly generated by the local packets. To further explore the local nonlinear energy transfer, the bicoherence analysis for the segment of the wave series with the freak wave appearance should be carried out. Figure 6 shows the wavelet bicoherence for the time

segment shown in Figure 4. It is seen that the degree of triad interaction and energy transfer is more evident than that occurring in the whole realization, further proving the higher harmonics are generated by local wave-wave interactions.

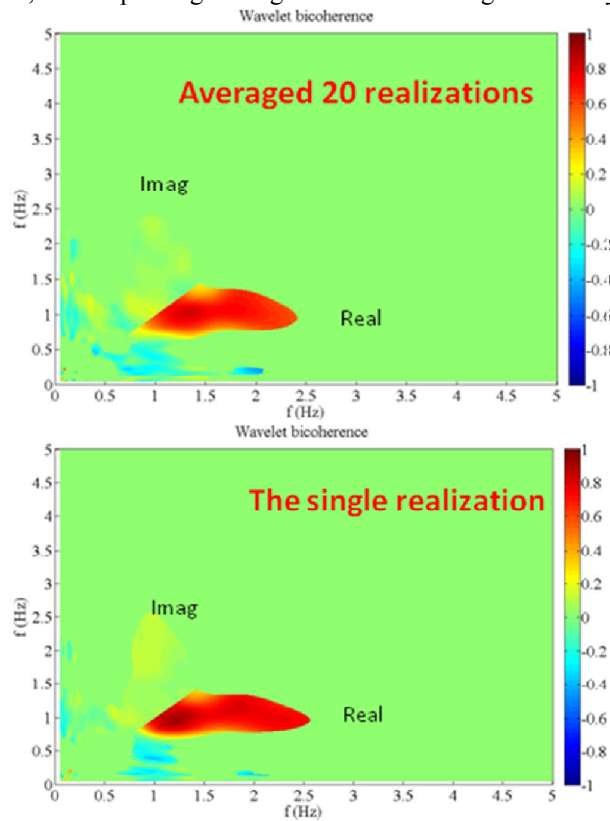


Figure 5. The wavelet-based bicoherence for the total 20 realizations (the upper panel) and for the single realization in which the freak wave in Figure 4 is identified (the lower panel).

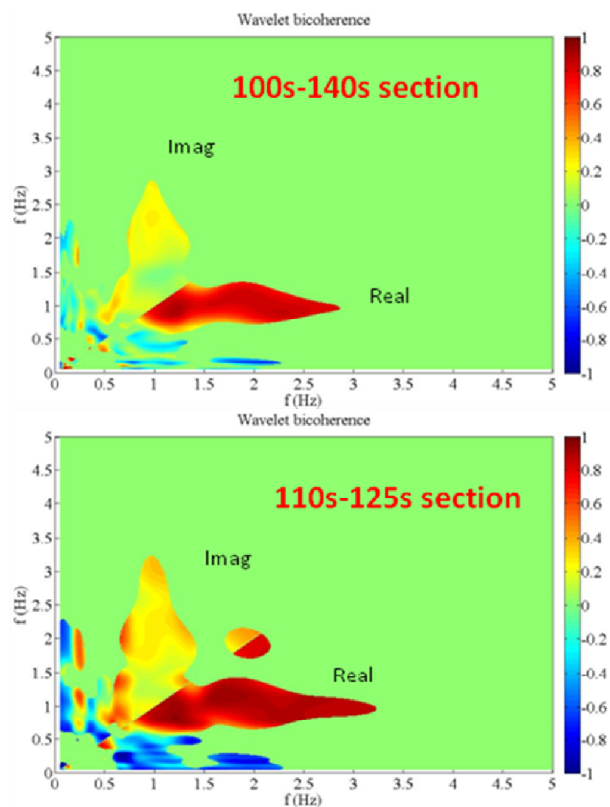


Figure 6. The wavelet-based bicoherence for the time segment 100s-140s of the wave series shown in Figure 4 (the upper panel) and for the time segment 110s-125s (the lower panel).

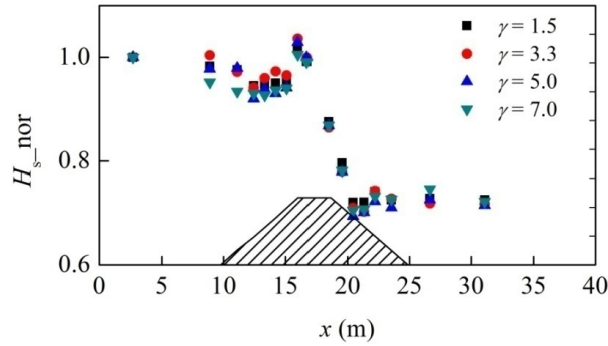


Figure 7. The variations of the normalized significant wave height along the wave flume.

The variations of the normalized significant wave heights for all the experimental cases are shown in Figure 7. It is shown that the wave heights decrease firstly due to the dissipation effect and then reach to the maximum at the top of the bar, then decrease rapidly in the deshoaling region. Meanwhile, the wave groupiness reaches to the maximum before the location with the maximum probability of occurrence of freak waves (Figure 8), indicating that the appearance of extreme waves relating to the groupiness of wave trains.

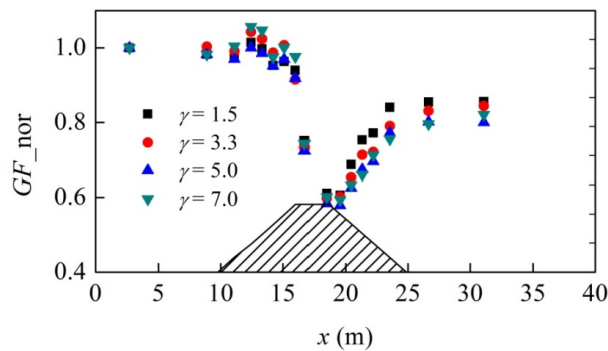


Figure 8. The variations of the normalized wave groupiness along the wave flume.

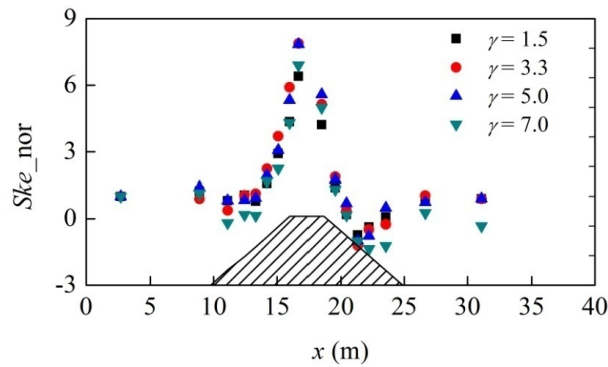


Figure 9. The variations of the normalized Skewness along the wave flume.

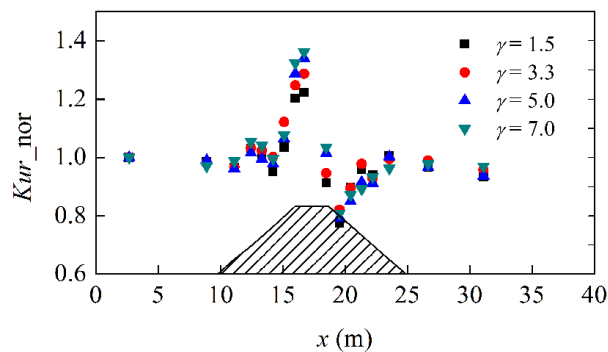


Figure 10. The variations of the normalized Skewness along the wave flume.

The variations of skewness and kurtosis are shown in Figures 9 and 10. Both the parameters approach to the maximum at the top of the bar near the upslope side, where behind the maximum probability occurrence of freak waves, suggesting that the parameters are not suitable as a index to predict the occurrence of freak waves. Additionally, the parameter kurtosis of the wave trains with narrower spectral bandwidth increase evidently in the shoaling process.

It is seemed that the skewness is correlated to the kurtosis. Based on the 3rd-order Stokes wave theory, Mori and Kobayashi (1998) derived a relationship between skewness and kurtosis for nearshore waves:

$$K = 3.0 + \left(\frac{4}{3}S\right)^2, \quad (11)$$

The relationship between the skewness versus kurtosis for the measured waves at different region is shown in Figure 11. It is shown that, the formula of Mori and Kobayashi (1998) fits well with the data measured on the upslope. In the deshoaling region, however, the relationship between skewness and kurtosis is around the Gaussian predication. On the crest of the bar, the formula clearly overestimated the kurtosis. A slight justification should be undertaken:

$$K = 2.1 + \left(\frac{4}{3}S\right)^2, \quad (12)$$

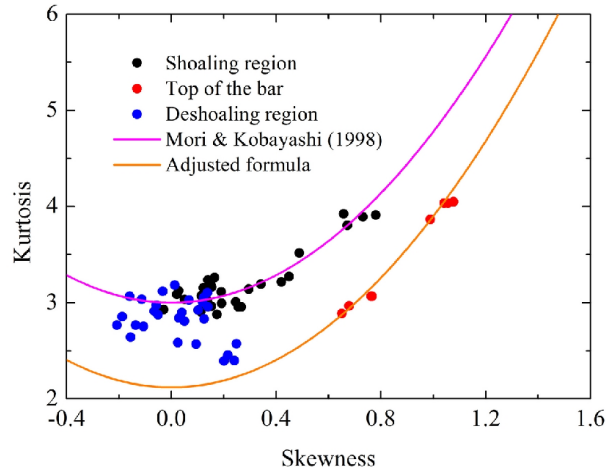


Figure 11. The relationship between skewness and kurtosis.

## Conclusions

A series of physical experiments on the variations of statistics of random waves propagating over a submerged bar were conducted. It is found that some distinct large waves (freak waves) are formed on the upslope side close to the top of the bar. Using the wavelet analysis method, these freak waves are mainly generated by the local triad wave-wave interactions. In addition, the appearance of freak waves is relating to the increasing of wave groupiness in the shoaling region. Furthermore, the relationship between the skewness and kurtosis in the shoaling region can be predicted well with the formula by Mori and Kobayashi (1998). However, on the top of the bar, the formula should be adjusted.

## ACKNOWLEDGMENTS

This research is supported financially by the National Nature Science Foundation (Grant Nos. 51109032, 11172058) and A Foundation for the Author of National Excellent Doctoral Dissertation of PR China (Grant No. 201347).

## REFERENCES

- Beji, S. and Battjes, J.A. 1993. Experimental investigation of wave propagation over a bar, *Coastal Engineering*, 19(1-2), 151-162.
- Chien, H., Kao, C.C. and Chuang, L.Z.H. 2002. On the characteristics of observed coastal freak waves, *Coastal Engineering Journal*, 44(4), 301-319.
- Dong, G.H., Ma, Y.X., Ma, X.Z. 2008. Cross-shore variations of wave groupiness by wavelet transform, *Ocean Engineering*, 35, 676-684.
- Dong, G.H., Ma, Y.X., Perlin, M., Ma, X.Z., Yu, B., Xu, J.W. 2008. Experimental study of wave-wave nonlinear interactions using the wavelet-based bicoherence, *Coastal Engineering*, 55, 741-752.
- Farge, M., 1992. Wavelet transforms and their applications to turbulence, *Annual Review of Fluid Mechanics*, 24, 395-457.
- Goda, Y. 2010. Random seas and design of maritime structures, Advanced Series on Ocean Engineering (33), World Scientific.
- Herbers, T.H.C., Russnogle, N.R., Elgar, S. 2000. Spectral energy balance of breaking waves within the surf zone, *Journal of Physical of Oceanography*. 30(11), 2723-2737.
- Kashima, H., Hirayama, K. and Mori, N. 2013. Numerical study of aftereffects of offshore generated freak waves shoaling to coast, *7th International Conference on Coastal Dynamics*.
- Katsardi, V., Lutio, L.de and Swan, C. 2013. An experimental study of large waves in intermediate and shallow water depths. Part 1: Wave height and crest height statistics, *Coastal Engineering*, 73, 43-57.

- Dysthe, K., Krogstad, H.E. and Müller, P., 2008, Oceanic Rogue Waves, *Annual Review of Fluid Mechanics*, 40, 287-310.
- Ma, Y.X., Dong, G.H., Liu, S.X., Zang, J., Li, J.X., Sun, Y.Y. 2010. Laboratory study of unidirectional focusing waves in intermediate depth water, *Journal of Engineering Mechanics*, 136 (1), 78-90.
- Mori, N. and Janssen, P.A.E.M. 2006. On Kurtosis and Occurrence Probability of Freak Waves, *Journal of Physical Oceanography*, 36(7), 1471-1483.
- Mori, N. and Kobayashi, N. 1998. Nonlinear distribution of nearshore free surface and velocity, *Proceeding of the 26th international conference of coastal engineering*, 189-202.
- Nikolkina, I., Didenkulova, I. 2011. Rogue waves in 2006-2010, *Natural Hazards and Earth System Sciences*, 11, 2913-2924.
- Trulsen, K., Zeng, H. and Gramstad, O. 2012. Laboratory evidence of freak waves provoked by non-uniform bathymetry, *Physics of Fluids*, 24, 097101.
- Zeng, H., Trulsen, K. 2012. Evolution of skewness and kurtosis of weakly nonlinear unidirectional waves over a sloping bottom, *Natural Hazards and Earth System Sciences*, 12, 631-638.
- Sergeeva, A., Pelinovsky, E. and Talipova, T. 2011. Nonlinear random wave field in shallow water: variable Korteweg-de Vries framework, *Natural Hazards and Earth System Sciences*, 11, 323-330.
- Torrence, C. and Compo, G.P. 1998. A practical guide to wavelet analysis, *Bulletin of American Meteorology Society*, 79 (1), 61-78.
- Wang, Y., Tao, A.F., Zheng, J.H., Doong, D.J., Fan, J., Peng, J. 2013. *Preliminary investigation on the coastal rogue waves of Jiangsu, China. Natural Hazards and Earth System Sciences*, doi:10.5194/nhessd-1-1-2013.